FISEVIER

Contents lists available at ScienceDirect

Thin-Walled Structures

journal homepage: www.elsevier.com/locate/tws



Full length article

Nonlinear thermoelastic fractional-order model of nonlocal plates: Application to postbuckling and bending response



Sansit Patnaik*, Sai Sidhardh, Fabio Semperlotti*

School of Mechanical Engineering, Ray W. Herrick Laboratories, Purdue University, West Lafayette, IN 47907, United States of America

ARTICLE INFO

Keywords: Fractional calculus Nonlocal elasticity Thermoelasticity Geometric nonlinearity Postbuckling Bending

ABSTRACT

This study presents a comprehensive frame-invariant fractional-order framework for the geometrically nonlinear bending and postbuckling analysis of nonlocal plates subject to combined thermal and mechanical loads. The fractional-order kinematic framework, unlike classical nonlocal formulations based on integerorder mechanics, is positive-definite and thermodynamically consistent. The positive-definite nature enables the application of variational principles to derive well-posed thermomechanical governing equations. A direct advantage of these theoretical advancements is reflected in the ability of the fractional-order approach to enable an energy-based asymptotic method obtained by extending the classical (local) Koiter's approach. This method allows the analytical assessment of the impact of nonlocal interactions on the nature of the bifurcation and post-critical response of slender structures when subject to compressive loads. Further, the positive-definite nature of the fractional-order approach allows the development of an accurate fractional-order finite element method enabling the simulation of nonlocal structures subject to any combination of thermomechanical loads and boundary conditions. The above stated advantages are particularly important for a comprehensive and consistent analysis of nonlocal structures in the postbuckling regime. The theoretical framework is used to provide analytical and numerical insights on the effect of combined thermal and mechanical loads on the nonlinear response of nonlocal plates. Numerical results also demonstrate the high-level consistency of the framework when applied to the nonlinear thermoelastic analysis of nonlocal plates under different loading and boundary conditions.

1. Introduction

The study of the response and the stability of structures subject to complex thermal and mechanical loads is a fundamental component of structural design and analysis in the most diverse field of engineering, biotechnology, and even medicine. Specific applications include, as an example, the design and analysis of lightweight aerospace and naval systems, sensors, biological implants and micro/ nano-electromechanical devices [1-5]. Typically, these systems are made of a combination of different slender structures and are subject to thermomechanical loads that can drive them into a geometrically nonlinear regime. Aerospace applications provide several practical examples where the combination of mechanical loads with the large and quickly varying aerodynamic and thermal loads can induce a strongly nonlinear response [2,6]. Similar examples can also be found in the design of micro/nano-electromechanical devices [7-10]. Experimental investigations have shown that, irrespective of the spatial scale, these slender structures tend to exhibit nonlocal (or size-dependent) effects in addition to the geometric nonlinearity. In fact, selected geometric designs have been connected to the occurrence of size effects in

several classes of structures [4,5,11,12]. Broadly speaking, in the case of macrostructures, nonlocal effects originate from material heterogeneities [3,13,14] and even intentionally nonlocal designs [4,12]. While interactions between the dissimilar material cells (e.g. periodic media) or layers (e.g. functionally graded materials) occur naturally in heterogeneous materials [3,13,14], these are induced artificially via specially designed short and/or long range connectors in the intentional nonlocal designs [4,12]. Although material heterogeneity and geometric effects also induce nonlocal effects in micro- and nano-structures, their contributions are less pronounced when compared to those from Van der Waals or nonlocal atomic interactions [10,11,15]. A detailed review on the origin, applications and modeling of nonlocal effects can be found in this recent study [16].

In the above mentioned applications, accuracy of predictions has critical impacts on the field deployment of these systems. The degree of accuracy of these predictions is strongly affected by the ability to model and account for both nonlinear and nonlocal effects in presence of thermomechanical loads, as well as for their complex interplay. The literature suggests that, despite the profound need for advanced

E-mail addresses: spatnai@purdue.edu (S. Patnaik), fsemperl@purdue.edu (F. Semperlotti).

Corresponding authors.

theories (and the corresponding numerical solvers) capable of modeling and simulating the nonlinear thermoelastic stability and response of higher-dimensional nonlocal structures, only a handful of studies are available [9,17-21]. None of these studies are based on the classical integral-based approach to nonlocal elasticity developed in [22]. Although few studies start from an integral approach, they evolve rapidly towards a simplified differential model using special exponential kernels [20,23]. As shown in [24,25], the differential models resulting from the use of special exponential kernels in the classical integral formulations are mathematically ill-posed (that is, the solution might not exist or it could exist but not being unique), resulting in inaccurate (often referred to as "paradoxical") predictions. The ill-posedness is a direct result of the inability of the model to achieve a positive-definite deformation energy [24]. Additionally, differential formulations face some difficulties when employed in dynamic analysis. As discussed in detail in [26], gradient based approaches require additional acceleration gradient terms in the constitutive formulation to ensure both well-posedness and causality. The above discussed limitations combined with the associated computational complexity and with the intrinsic thermodynamic inconsistency of the formulation [27,28] also prevents development of an energy-based approach for the nonlinear thermoelastic analysis of nonlocal structures. The lack of an energybased approach prevents the development of finite element models to numerically simulate the nonlinear systems under the most general combination of external loads. In fact the necessity of finite element based solvers follows also from the unparalleled flexibility of finite element solvers in treating integral boundary conditions, typical of nonlocal models [24,25,29,30]. Additionally, the development of finite element based solvers for postbuckling analysis (both mechanical and thermomechanical) is essential. Indeed, the lack of an energybased approach also prevents the application of analytical methods (particularly, asymptotic techniques [31,32]) to determine the effect of nonlocality, and of thermal and mechanical loads on the nature of both bifurcation and post-critical response. In this study, we address the above discussed conceptual and practical limitations of the classical nonlocal approaches by leveraging a fractional calculus based formulation. We will analyze the specific advantages of the proposed approach and illustrate how the proposed method is highly suitable for nonlinear thermomechanical analysis of slender nonlocal structures.

Fractional calculus is rapidly emerging as a powerful mathematical tool that is particularly well-suited to model complex phenomena characterized by nonlocal effects. The differ-integral definition of fractional operators provides a natural way to account for nonlocal effects, as first highlighted in the seminal work on fractional-order continuum mechanics by Lazopoulos [33]. This initial study was rapidly followed by many other researchers that developed a variety of fractional-order-based approaches to nonlocal elasticity. These different approaches differentiated from each other either based on the rationale for the introduction of the fractional-order operator within the classical continuum mechanics formulation or on the process adopted to develop the fractionalorder equilibrium equations describing the nonlocal continua. Concerning the former difference, the majority of the early formulations were based on fractional-order stress-strain relations [5,33-36] while more recent formulations adopt fractional-order strain-displacement (kinematic) relations [14,37-41]. Further, the different methods developed the fractional-order equilibrium equations for nonlocal continuum either by employing a Newtonian equilibrium approach [5,33-38] or by means of variational principles [39,41].

While each fractional-order nonlocal continuum model presents interesting insights into the response of nonlocal solids, the model based on fractional-order kinematics and formulated using variational principles leads to a frame-invariant formulation having significant theoretical and practical advantages over existing integer-order nonlocal models [39–43]. First, the fractional-order kinematic approach guarantees a positive-definite deformation energy density. Consequently, the nonlocal (fractional-order) governing equations derived from the deformation energy, via variational minimization of the system's energy, are

well-posed in nature and lead to consistent predictions free from boundary effects. This result is in sharp contrast to the integer-order strain driven approaches which do not guarantee a positive-definite deformation energy and lead to ill-posed formulations that could potentially lead to inaccurate predictions [24,25]. Although the ill-posed nature of the strain-driven integral approach was addressed via a stress-driven approach [25], the stress-driven approach relies on analytical methods for a simulation of the nonlocal response [25,30]. This aspect limits the application of the stress-driven approach particularly when approaching higher dimensional (2D or 3D) nonlocal structures and finite displacement (nonlinear) analyses. On the contrary, the fractionalorder kinematic approach is amenable to finite element simulations and enables a direct incorporation of finite (nonlinear) displacements [42, 43], thanks to the positive-definite nature of the formulation. In addition to the mathematical well-posedness, the fractional-order kinematic approach is thermodynamically consistent. The fractional-order kinematic relations allow a point-wise enforcement of both the first and the second thermodynamic balance laws within the domain of the nonlocal solid. This observation is in sharp contrast to the classical integral approaches that allow the thermodynamic balance laws to be satisfied only in an integral (i.e. weak) sense, hence leading to physical inconsistencies [28]. The mathematical and thermodynamic consistency of the fractional-order formulation allows using asymptotic techniques, rooted in an energy-based approach, to analytically examine the nature of both bifurcation and post-critical response, as well as the impact of different fractional-order constitutive parameters on the same aspects. In view of the above discussion, and of the fact that the fractionalorder kinematic approach leads to frame invariance, well-posedness, thermodynamic consistency, ability to incorporate nonlinear effects and to admit finite element techniques, it appears that this approach holds a significant potential to study the nonlinear stability and response of slender nonlocal structures subject to thermomechanical loads.

The present study has two major objectives. First, we develop a fractional calculus based framework to analyze the geometrically nonlinear thermoelastic stability and response of nonlocal plates. For this purpose, we extend the fractional-order geometrically nonlinear formulation proposed in [42] and the fractional-order thermoelastic constitutive modeling proposed in [43] to account for the postbuckling and nonlinear bending response of nonlocal plates subject to thermomechanical loads. For the postbuckling analysis, we also make use of the stability studies of fractional-order nonlocal structures conducted in [44] and of Koiter's asymptotic method [31,32] to provide some analytical insights on the nature of the bifurcation at the critical point and the stability of the bifurcated curves. In fact, the current study also extends the purely mechanical postbuckling analysis of nonlocal structures conducted in [45] to shear deformable plates subject to combined thermomechanical loads. In this regard, note that the fractional-order model proposed in this study is based on the classical (local) Mindlin plate formulation. This selection makes the current study more general and complete since the Kirchhoff plate formulation studied in [45] can be recovered as a special case from the formulation presented in this study. Second, we use the fractional-order finite element method (f-FEM) developed in [41,42] to numerically solve the nonlinear thermoelastic model. We analyze the effect of different thermal and mechanical loading conditions, and of the fractional-order constitutive parameters on the postbuckling and nonlinear bending response of the nonlocal plates.

2. Fractional-order thermoelastic formulation of nonlocal solids

The nonlinear thermomechanical formulation presented in this section builds upon the fractional-order nonlocal continuum formulation developed in a series of previous studies [14,40–42]. The thermodynamic consistency of the fractional-order nonlocal continuum was analyzed in [43] and the linear stability analysis of nonlocal structures, modeled by the fractional-order approach, was presented in [44]. In

this section, we build upon these thermoelastic and stability studies, to formulate a comprehensive thermoelastic formulation to analyze the nonlinear bending and postbuckling response of nonlocal structures subject to combined thermomechanical loads. We will first recall (briefly) the thermomechanical constitutive model of nonlocal solids and then extend this framework to analyze the stability of nonlocal structures modeled via the fractional-order approach. More specifically, we will analyze the effect of thermomechanical loads on both critical points and post-critical response of the nonlocal solids.

2.1. Thermoelastic constitutive modeling

According to the fractional-order kinematic approach, the strain in the nonlocal medium is defined using a fractional-order analogue of the classical (local) deformation gradient tensor. The geometrically nonlinear Eulerian strain tensor obtained by this approach is given as [14.40]:

$$\varepsilon = \frac{1}{2} \left(\nabla_x^{\alpha} \mathbf{u} + \nabla_x^{\alpha} \mathbf{u}^T + \nabla_x^{\alpha} \mathbf{u} \nabla_x^{\alpha} \mathbf{u}^T \right) \tag{1}$$

where u(x) is the displacement field. The fractional-order gradient of the displacement field in deformed coordinates x, denoted by $\nabla_x^\alpha u$, is defined as $\nabla_x^\alpha u = D_{x_j}^\alpha u_i$. The term $D_{x_j}^\alpha u_i$ is a space-fractional Riesz–Caputo (RC) derivative with the fractional-order $\alpha \in (0,1]$ and interval $x_j \in (x_{A_j}, x_{B_j})$, and is defined as [14]:

$$D_{x_j}^{\alpha}u_i(\boldsymbol{x},t) = \frac{1}{2}\Gamma(2-\alpha)\left[l_{A_j}^{\alpha-1}\begin{pmatrix} C \\ x_{A_j} D_{x_j}^{\alpha}u_i(\boldsymbol{x},t) \end{pmatrix} - l_{B_j}^{\alpha-1}\begin{pmatrix} C \\ x_j D_{x_{B_j}}^{\alpha}u_i(\boldsymbol{x},t) \end{pmatrix}\right]$$
(2)

where $\Gamma(\cdot)$ is the Gamma function. $\frac{C}{x_{A_j}}D^{\alpha}_{x_j}u_j$ and $\frac{C}{x_j}D^{\alpha}_{x_{B_j}}u_j$ are the left- and right-handed fractional-order Caputo derivatives of u_j , respectively. As evident from the above equation, the fractional-order formulation introduces two parameters: the fractional-order and the interval of the RC derivative. Although it appears from Eq. (2) that the length-scales $(I_{A_j}$ and $I_{B_j})$ are additional parameters, they are directly related to the interval of the RC derivative. A brief discussion on the physical significance of these different fractional-order constitutive parameters is provided in the following:

- Role of the fractional-order α : The RC derivative consists of a power-law kernel $\kappa(x_j,x_j')=1/|x_j-x_j'|^\alpha$ with support being equal to the interval of the derivative (x_{A_j},x_{B_j}) . This power-law kernel models the strength of interaction between particles separated by a distance, but contained within that interval. The fractional-order $\alpha\in(0,1]$ is the exponent of the power-law kernel and determines the spatial rate of decay of the nonlocal interactions.
- Role of the interval of the RC derivative: The interval of the leftand right-handed derivatives correspond to the support of the power-law kernel of each derivative, and hence it determines the distance beyond which two particles no longer interact via long-range forces. Physically, this represents the horizon of nonlocality.
- *Role of the length-scales:* The length-scales serve a dual purpose; they ensure that the formulation is dimensionally consistent, and more importantly, frame-invariant. For this latter purpose, it is required that $l_{A_j} = x_j x_{A_j}$ and $l_{B_j} = x_{B_j} x_j$ [14]. Note that $x_{B_j} x_{A_j} = l_{A_j} + l_{B_j}$. It immediately follows that the length scales determine the dimensions of the horizon of nonlocality on either side of a point x along a given direction. In general, the length scales l_{A_j} and l_{B_j} are independent parameters such that $l_{A_j} \neq l_{B_j}$ suggesting that the formulation can model an *asymmetric* horizon (see Fig. 1). This capability is particularly relevant for material boundaries and even interfaces between different materials, where it enables an exact treatment of frame-invariance. From a more physical perspective, the asymmetry in the horizon that is

achieved via a truncation of the length scales (or equivalently, a truncation of the horizon of nonlocality), allows accounting for the long-range interactions (at an atomistic or molecular level) that are broken due to the presence of material and/or geometric discontinuities [46].

For better visualization, we have illustrated the two different fractionalorder constitutive parameters in Fig. 1. A more detailed mathematical treatment of the above aspects can be found in [14].

The fractional-order approach presents a net departure from classical approaches to nonlocal elasticity. Contrary to classical approaches that model nonlocality via stress–strain constitutive relations, the fractional-order approach adopts a kinematic route to capturing the effect of the nonlocality. In the fractional-order kinematic approach, nonlocality is modeled via fractional-order strain–displacement relations (see Eq. (1)). This starting point has significant implications on the resulting theory. Apart from ensuring a positive-definite, stable and well-posed formulation, the fractional-order kinematic relations guarantee a strong (localized) imposition of the first and second laws of thermodynamics at each point within the continuum [39,43]. This thermodynamic consistency of the fractional-order approach allows the derivation of localized material constitutive relations from the thermodynamic balance laws [43]:

$$\sigma_{ij} = \frac{\partial \psi}{\partial \varepsilon} \tag{3a}$$

$$\eta = -\frac{\partial \psi(\varepsilon, \theta)}{\partial \theta} \tag{3b}$$

where σ_{ij} is the stress tensor, ψ is the Helmholtz free energy, and η is the entropy of the nonlocal solid. Recall that the Helmholtz free energy $\psi(\varepsilon,\theta)$ is a function of the following independent variables: (1) the fractional-order strain ε , and (2) the temperature difference $\theta = T - T_0$, where T and T_0 are the temperature field distribution within the solid and the ambient temperature, respectively. The Helmholtz free energy in isotropic nonlocal solids, modeled using the fractional-order approach, is derived from first principles in [43] as:

$$\psi(\epsilon, \theta) = \frac{1}{2} \lambda \epsilon_{kk} \epsilon_{ll} + \mu \epsilon_{ij} \epsilon_{ij} - (3\lambda + 2\mu) \alpha_0 \epsilon_{kk} \theta - \frac{C_v^0}{2T_0} \theta^2$$
 (4)

where λ and μ are the Lamé parameters, C_v^0 is the specific heat at constant strain, and α_0 is the coefficient of thermal expansion. All the above defined material properties are defined at ambient temperature T_0 . By substituting the expression for the Helmholtz free energy in Eq. (3), the constitutive relations for an isotropic nonlocal elastic solid are obtained as:

$$\sigma_{ii}(\varepsilon,\theta) = \lambda \delta_{ii} \varepsilon_{kk} + 2\mu \varepsilon_{ii} - (3\lambda + 2\mu)\alpha_0 \delta_{ii}\theta$$
 (5a)

$$\eta(\varepsilon,\theta) = (3\lambda + 2\mu)\alpha_0 \varepsilon_{kk} + \frac{C_v^0}{T_0} \theta$$
 (5b)

We highlight that, although the focus of this study is on modeling an isotropic nonlocal solid, the formulation presented is general and any type of solid (e.g. orthotropic or anisotropic) can be modeled via appropriate changes in the above constitutive equations.

2.2. Thermomechanical postbuckling of nonlocal structures

The stability analysis of a given structure involves the application of the Lagrange–Dirichlet theorem which involves a minimization of the total potential energy of the structure. The classical integer-order theories of nonlocal elasticity do not allow the direct application of the Lagrange–Dirichlet theorem since they do not ensure a positive-definite deformation energy (or a positive semi-definite potential energy) [24,25,39]. This characteristic highlights a practical advantage of

Fig. 1. Schematic illustration of the physical significance of the fractional-order parameters: (a) the fractional-order α , and (b) the length scales. The fractional-order α in (a), which is obtained as the slope of the logarithm of the power-law kernel of the fractional derivative: $\kappa(x,x') = 1/|x-x'|^{\alpha}$, determines the strength of the nonlocal interaction between a fixed point x and points in its horizon of nonlocality. The length scales in (b) illustrate the horizon of nonlocality at different points in the 2D domain. Note that the horizon of nonlocality at the point x_2 is equal to t_f on either sides in the \hat{x} direction. On the contrary, the horizon of nonlocality at x_1 and x_3 is truncated ($t_f^{\dagger} < t_f$) on the left and right sides, respectively.

the fractional-order approach which guarantees a positive-definite deformation energy and therefore allows the application of the Lagrange–Dirichlet theorem [39,41]. The total potential energy of a nonlocal solid is given as [39]:

$$\Pi[\mathbf{u}(\Lambda)] = \frac{1}{2} \int_{\Omega_{\epsilon}} \boldsymbol{\sigma} : \epsilon dV - \int_{\Omega_{\epsilon}} F(\Lambda) \cdot \mathbf{u} dV$$
 (6)

where Ω_s denotes the domain of the nonlocal solid, and dV denotes the differential volume. Further, $F(\Lambda)$ is an external force applied on the solid and Λ is a continuous variable which is used as the control parameter to characterize the adjacent states of equilibrium. While this parameter-controlled force vector has clear physical interpretations for purely mechanical loads, an analogous interpretation also holds for thermal loads. Recall that, in order to generate instability, in-plane stresses are required within the slender structure [32]. This is achieved, for example, via in-plane (or surface) loads in purely mechanical analysis [45]. However, even in the absence of external mechanical loads, in-plane stresses can be generated by thermal loads. Analogous to mechanical loads, a control parameter (such as, for example, θ or the gradient of θ) can be defined. In this regard, note that the thermal field variable, that is θ , is captured in the nonlocal stress σ via Eq. (13). In fact, the thermal and mechanical loads can also be combined, allowing for the definition of more general control parameters. In conclusion, we note that irrespective of the nature of the loading (thermal and/or mechanical) these instability-inducing control factors can be combined within the parameter-controlled force vector in order to analyze the stability of any given structure [18,19,47].

Recall that the equilibrium equations describing a given structure are obtained from the first variation of the potential energy in the direction of u, that is, $\delta \Pi[\mathbf{u}(\Lambda)]_{,u} = \Pi_{,u}\delta u$. More specifically, for an equilibrium state $u_e(\Lambda_e)$, we have [44]:

$$\int_{\Omega_{s}} \sigma : \left[\varepsilon^{(l)}(\delta \mathbf{u}) + \varepsilon^{(n)} \left(\mathbf{u}_{e}, \delta \mathbf{u} \right) \right] dV - \int_{\partial \Omega^{s}} F(\Lambda_{e}) \cdot \delta \mathbf{u} dA = 0$$
 (7)

for any arbitrary variation δu . In the above equation, $\varepsilon^{(l)}=1/2(\nabla_x^\alpha u+\nabla_x^\alpha u^T)$ denotes the linear part of the nonlocal strains and $\varepsilon^{(n)}=1/2(\nabla_x^\alpha u\nabla_x^\alpha u\nabla_x^\alpha u^T)$ denotes the geometrically nonlinear part of the nonlocal strains. At a first glance, thermal field variables appear to be absent in the Eq. (7). However, one should recall that the thermal load is captured within the nonlocal stress via Eq. (13). Further, in the above equation as well as in the subsequent discussion, we have assumed that the temperature distribution across the nonlocal solid is available *a priori*, that is as an input to the problem. This implies that the independent variation of the temperature field $\delta\theta=0$. Therefore, the application of variational principles leads to an independent variation of the displacement field alone.

The equilibrium configuration $u_e(\Lambda_e)$ described via Eq. (7) is stable iff the second-variation $\delta^2 \Pi[u_e(\Lambda_e)] = \Pi_{,uu} \delta u_1 \delta u_2 > 0$, where δu_1 and δu_2 are independent variations. The critical configuration of stability

that is $u_c(\Lambda_c)$, can now be obtained as the solution to the following variational equation $\delta^2 H[u_c] = 0$ [44]:

$$\int_{\Omega} \left[\left[\boldsymbol{\varepsilon}^{(l)} (\delta \boldsymbol{u}_{2}) + \boldsymbol{\varepsilon}^{(n)} \left(\boldsymbol{u}_{c}, \delta \boldsymbol{u}_{2} \right) \right] : \mathbf{C} : \left[\boldsymbol{\varepsilon}^{(l)} (\boldsymbol{u}_{b}) + \boldsymbol{\varepsilon}^{(n)} \left(\boldsymbol{u}_{c}, \boldsymbol{u}_{b} \right) \right]
+ \Lambda_{c} \boldsymbol{\sigma}^{0} : \boldsymbol{\varepsilon}^{(n)} \left(\delta \boldsymbol{u}_{2}, \boldsymbol{u}_{b} \right) \right] dV = 0$$
(8)

where $u_h = \delta u_1$ is the critical mode corresponding to the bifurcation at u_c . In deriving the above expression, a proportional loading force $(F(\Lambda) = \Lambda F^0$, with F^0 being a representative force vector) is assumed; the resulting state of stress is $\sigma(\Lambda) = \Lambda \sigma^0$. We merely note that the above assumption of a proportional stress corresponding to a proportional loading force holds true for purely mechanical, purely thermal, and combined thermomechanical loads (all controlled via the same parameter Λ). To account for combined thermal and mechanical loads subject to separate load control parameters, some additional terms would appear in the variational Eq. (8). In the following, we do not consider this latter case since it adds to the complexity of the equations without affecting the generality of the conclusions. Note that these are common assumptions in classical stability analysis [32]. Further details including the derivation of the above expression and of the linearized critical points (for a purely mechanical case) can be found in [44]. We do not discuss the latter aspect, since we solve the fully nonlinear governing equations while the response evolves towards the postbuckling regime, by adopting an energy-based approach. While the energy-based approach allows the numerical simulation of the postbuckling response, some qualitative insights on the postbuckling response of the nonlocal solid is necessary. For this purpose we extend Koiter's asymptotic method [31], initially formulated for the postbuckling response of classical (local) structures, to the fractional-order formulation.

A perturbation around the critical configuration (u_c, Λ_c) can be expressed using Koiter's method as [31,32]:

$$\Lambda - \Lambda_c = \chi \Lambda_1 + \frac{1}{2} \chi^2 \Lambda_2 + \frac{1}{6} \chi^3 \Lambda_3 + h.o.t$$
 (9a)

$$\boldsymbol{u} - \boldsymbol{u}_c = \tilde{\boldsymbol{u}} = \chi \boldsymbol{u}_b + \underbrace{\frac{1}{2} \chi^2 \boldsymbol{w}_2 + \frac{1}{6} \chi^3 \boldsymbol{w}_3}_{\mathbb{W}(\chi)} + h.o.t$$
 (9b)

where χ is a parameter within the expansion, and $\tilde{\boldsymbol{u}}$ is the difference between the fundamental curve C_0 (for $\Lambda < \Lambda_c$) and the bifurcated curve C_0^* (for $\Lambda \geq \Lambda_c$). As evident from Eqs. (9), Koiter's method allows us to express this difference in terms of the critical mode \boldsymbol{u}_b obtained in Eq. (8) and a correction factor \mathbb{W} defined such that $\mathbb{W} \perp \boldsymbol{u}_b$. Further, the set of expansion coefficients $\{\boldsymbol{u}_b, \Lambda_1\}$ and $\{\boldsymbol{w}_2, \Lambda_2\}$ are physically interpreted as the slope and curvature of the load–displacement equilibrium curves at the point $\chi=0$, respectively [32]. Along the fundamental path C_0 , $\delta^2 \boldsymbol{\Pi}$ is positive indicating a stable equilibrium. With increase in the value of Λ along the forward direction of C_0 , $\delta^2 \boldsymbol{\Pi}$ reduces and finally at the critical point Λ_c we have $\delta^2 \boldsymbol{\Pi}_c=0$. By assuming the independent variation $\delta \boldsymbol{u}_2=\tilde{\boldsymbol{u}}$ in Eq. (8) we obtain that [32]:

$$\mathcal{R} = \frac{\mathrm{d}[\delta^2 \Pi_c]}{\mathrm{d}\Lambda} = \int_{\Omega} \sigma^0 : \varepsilon^{(n)}(\tilde{\mathbf{u}}, \tilde{\mathbf{u}}) \mathrm{d}\Omega$$
 (10)

where \mathcal{R} is the *transversality rate*. Further, the perturbation (or, difference) in the potential energy between the two configurations on the fundamental curve C_0 and the bifurcated curve C_0^* , for a given value of Λ , can be expressed using the asymptotic expansion and the transversality rate in Eqs. (9), (10) as [48]:

$$\Delta \Pi = \Pi(C_0^*) - \Pi(C_0) = \begin{cases} \frac{1}{6} \Lambda_1 \mathcal{R} \chi^3 + \mathcal{O}(\chi^3) + h.o.t & \text{if } \Lambda_1 \neq 0 \\ \frac{1}{24} \Lambda_2 \mathcal{R} \chi^4 + \mathcal{O}(\chi^4) & \text{if } \Lambda_1 = 0 \text{ and } \Lambda_2 \neq 0 \end{cases}$$

The expressions for the transversality rate in Eq. (10) and the potential energy difference in Eq. (11) lead to the following important observations on the nature of the bifurcation, the stability of the bifurcated curves of the nonlocal structure, and the effect of the fractional-order constitutive parameters:

- For $\Lambda > 0$, the term $\varepsilon^{(n)}(\tilde{u}, \tilde{u})$ is quadratic and nonzero. Further, σ^0 is either positive or negative (or equivalently, tensile or compressive) depending on the nature of the force vector F^0 or the thermal load. Hence, it follows from Eq. (10) that $\mathcal{R} \neq 0$. As established in literature, a nonzero value of R indicates an angular bifurcation at the critical point [31,32]. It immediately follows that the fundamental equilibrium curve C_0 , obtained via the fractional-order approach, undergoes an angular bifurcation at the critical point. Note that the angular bifurcation phenomenon occurs irrespective of the specific values of the fractional-order constitutive parameters and is also consistent with classical (local) studies [32]. We merely note that this angular bifurcation is assumed in studies conducted on postbuckling response of nonlocal structures via integer-order models without any formal proof [7,9, 47]. It is noteworthy that the energy-based approach, afforded by the positive-definite fractional-order formulation, allows reaching a concrete proof of angular bifurcation at the critical point (as shown above).
- Note from Eq. (8) that the critical point corresponds to a negative value for σ_0 [32,44]. In other terms, a compressive force F_0 or a thermal load causing $\sigma^0 < 0$ is required to induce an instability within the nonlocal structure, consistent with classical formulations as well as experimental evidence. Consequently, it follows from Eq. (10) that $\mathcal{R} < 0$.
- For $\mathcal{R}<0$, it follows from Eq. (11) that $\Delta \Pi<0$. Thus, equilibrium configurations along the bifurcated curve C_0^* admit lower potential energy than the fundamental branch for $\Lambda>\Lambda_c$. It follows that the bifurcated branch at the critical point Λ_c presents stable equilibrium solutions for $\Lambda>\Lambda_c$. We note that numerical simulations via the energy approach are expected to yield only the stable branches.
- · Although the degree of nonlocality (that is, the specific values of the fractional-order constitutive parameters) has no effect on the nature of the bifurcation, it does affect the shape of the bifurcated curve. In this regard, note that a decrease in the value of the fractional-order and/or an increase in the value of the length-scales (physically indicating an increase in the degree of nonlocality) would result in lower values of the fractional derivatives, hence indicating a softening effect [39,41]. It follows that the numerical values of σ^0 and $\varepsilon^{(n)}(\tilde{u}, \tilde{u})$ in Eq. (10) will be reduced resulting in a lower value of R with increasing degree of nonlocality [44]. It immediately follows from Eq. (11) that an increasing degree of nonlocality reduces the difference in the energy barrier between the fundamental and the bifurcated paths (for the same control parameter Λ), beyond the critical point. This indicates a higher degree of instability in the nonlocal structure as a result of the softening effects. We will demonstrate this aspect numerically in Section 4.

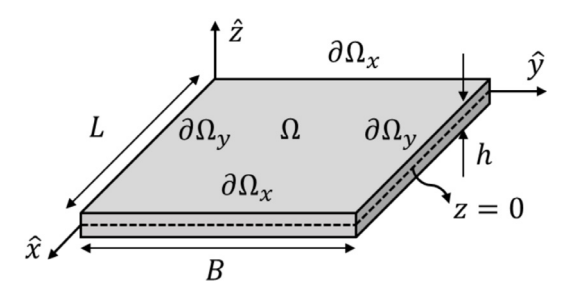


Fig. 2. Schematic of a rectangular plate indicating the basic geometric parameters along with the chosen Cartesian reference frame.

3. Thermoelastic fractional-order Mindlin theory of plates

The fractional-order nonlocal continuum formulation described in Section 2 was used to analyze the response of nonlocal plates via a fractional-order Mindlin formulation in [41,42]. Note that the study conducted in [41] focused on the linear response, while the study conducted in [42] focused on the nonlinear response. In the present study, we leverage the nonlinear formulation presented in [42] and the concepts of fractional-order thermoelasticity reviewed in Section 2.1, to develop a comprehensive nonlinear thermoelastic formulation that enables the analysis of combined thermomechanical loads on the nonlinear bending and postbuckling response of nonlocal plates.

A schematic of the undeformed rectangular plate along with the chosen Cartesian reference frame is illustrated in Fig. 2. The length, width, and thickness of the plate are given as L, B and h, respectively. The mid-plane of the plate, identified as z=0, is denoted as Ω and its edges are denoted as $\{\partial\Omega_x,\partial\Omega_y\}$. According to the Mindlin plate theory, the in-plane components (u(x,t)) and v(x,t) and transverse component (w(x,t)) of the displacement field at a spatial location x(x,y,z) are related to the displacements of the mid-plane Ω in the following manner [49]:

$$u(\mathbf{x},t) = u_0(x,y,t) - z\theta_x(x,y,t)$$
(12a)

$$v(\mathbf{x},t) = v_0(x,y,t) - z\theta_v(x,y,t)$$
(12b)

$$w(\mathbf{x},t) = w_0(x,y,t) \tag{12c}$$

where u_0 , v_0 , and w_0 denote the displacements at the mid-plane of the plate along the \hat{x} , \hat{y} , and \hat{z} directions. θ_x and θ_y denote the rotations of the transverse normal at the mid-plane of the plate, about the \hat{y} and \hat{x} axes, respectively. In the following, for a compact notation, we will not specify the functional dependence of the displacement fields on the spatial and temporal variables.

By using the displacement field in Eq. (12), and then assuming moderate rotations of the transverse normals $(10^{\circ}-15^{\circ})$ and small displacement gradients, the nonlinear von-Kármán strain–displacement relations for the plate can be derived from the Eulerian strain tensor definition in Eq. (1) as [42]:

$$\varepsilon_{xx} = D_x^{\alpha} u_0 + \frac{1}{2} (D_x^{\alpha} w_0)^2 - z D_x^{\alpha} \theta_x$$
 (13a)

$$\varepsilon_{yy} = D_y^{\alpha} v_0 + \frac{1}{2} (D_y^{\alpha} w_0)^2 - z D_y^{\alpha} \theta_y$$
(13b)

$$\gamma_{xy} = D_y^{\alpha} u_0 + D_x^{\alpha} v_0 + D_x^{\alpha} w_0 D_y^{\alpha} w_0 - z (D_y^{\alpha} \theta_x + D_x^{\alpha} \theta_y)$$
 (13c)

$$\gamma_{xz} = D_x^{\alpha} w_0 - \theta_x \tag{13d}$$

$$\gamma_{vz} = D_v^{\alpha} w_0 - \theta_v \tag{13e}$$

It follows from Eq. (12c) that the transverse strain $\varepsilon_{zz}=0$, which is consistent with the first-order local shear deformation theory [49]. Note that, unlike the in-plane strains, the transverse shear strains do not show a nonlocal dependence on the rotations of the mid-plane of the plate. This is a direct consequence of the fact that, in the Mindlin formulation, the displacement degrees of freedom $(\{u_0,v_0,w_0,\theta_x,\theta_y\})$ are assumed to be constant across the thickness of the plate and the response of the plate is solely described by the mid-plane of the plate (see Eq. (12)). From a physical perspective, the effect of the nonlocal interactions across the thickness of the slender plate are negligible when compared to the nonlocal interactions across its plane. Using the fractional-order nonlinear strains in Eq. (13), the nonlocal stresses generated in an isotropic plate due to thermomechanical loads are obtained from Eq. (5) as:

$$\sigma_{xx} = \frac{E}{1 - v^2} \left[\varepsilon_{xx} + v \varepsilon_{yy} - (1 + v) \alpha_0 \theta \right]$$
 (14a)

$$\sigma_{yy} = \frac{E}{1 - v^2} \left[v \epsilon_{xx} + \epsilon_{yy} - (1 + v) \alpha_0 \theta \right]$$
 (14b)

$$\{\sigma_{xy}, \sigma_{xz}, \sigma_{yz}\} = \frac{E}{2(1+y)} \{\gamma_{xy}, \gamma_{xz}, \gamma_{yz}\}$$
 (14c)

where E is the Young's modulus and ν is the Poisson's ratio of the isotropic solid.

By using the above defined stress and strain fields, induced in the nonlocal plate due to the thermomechanical loads, the deformation energy \mathbb{U} , the work done by external forces \mathbb{V} , and the kinetic energy \mathbb{T} of the plate are obtained as:

$$\mathbb{U} = \int_{\Omega} \int_{-\frac{h}{2}}^{\frac{h}{2}} \left[\sigma_{xx} \epsilon_{xx} + \sigma_{yy} \epsilon_{yy} + \sigma_{xy} \gamma_{xy} + \sigma_{xz} \gamma_{xz} + \sigma_{yz} \gamma_{yz} \right] dz d\Omega$$
 (15a)

$$\mathbb{V} = \int_{\Omega} \left[F_x u_0 + F_y v_0 + F_z w_0 + M_{\theta_x} \theta_x + M_{\theta_y} \theta_y \right] d\Omega
+ \int_{\partial \Omega_v \cup \partial \Omega_v} \left[\hat{F}_x u_0 + \hat{F}_y v_0 + \hat{F}_z w_0 + \hat{M}_{\theta_x} \theta_x + \hat{M}_{\theta_y} \theta_y \right] d\partial\Omega$$
(15b)

$$\mathbb{T} = \int_{\Omega} \int_{-\frac{h}{2}}^{\frac{h}{2}} \rho \left[\left(\dot{u}_0 - z \dot{\theta}_x \right) \left(\dot{u}_0 - z \dot{\theta}_x \right) + \left(\dot{v}_0 - z \dot{\theta}_y \right) \left(\dot{v}_0 - z \dot{\theta}_y \right) + \dot{w}_0 \dot{w}_0 \right] dz d\Omega \tag{15c}$$

where ρ denotes the mass density of the plate. Note that $d\Omega = dxdy$ for a rectangular plate. $\{F_x, F_y, F_z\}$ are the loads applied externally in the \hat{x} , \hat{y} , and \hat{z} directions, respectively on the mid-plane of the plate. $\{M_{\theta_x}, M_{\theta_y}\}$ are the moments applied about the \hat{y} and \hat{x} axes, respectively on the mid-plane of the plate. Similarly, $\{\hat{F}_x, \hat{F}_y, \hat{F}_z, \hat{M}_{\theta_x}, \hat{M}_{\theta_y}\}$ denote the external loads and moments applied on the boundaries of the plate. The strong-form of the governing equations can now be derived by using the extended Hamilton's principle:

$$\int_{t_1}^{t_2} (\delta \mathbb{U} - \delta \mathbb{V} - \delta \mathbb{T}) \, \mathrm{d}t = 0 \tag{16}$$

The simplification of Eq. (16) follows standard principles of fractional variational calculus. In the following, we directly report the strong-form of the geometrically nonlinear thermoelastic governing equations and refer the interested reader to [39,42,43] for the details of the variational simplifications.

The governing equations for the thermoelastic response of the non-local plate are:

$$\mathfrak{D}_x^{\alpha} N_{xx} + \mathfrak{D}_y^{\alpha} N_{xy} + F_x = \rho h \frac{\partial^2 u_0}{\partial t^2}$$
 (17a)

$$\mathfrak{D}_{x}^{\alpha}N_{xy} + \mathfrak{D}_{y}^{\alpha}N_{yy} + F_{y} = \rho h \frac{\partial^{2}v_{0}}{\partial t^{2}}$$
(17b)

 $\mathfrak{D}_{x}^{\alpha}(Q_{xz}+N_{xx}D_{x}^{\alpha}w_{0}+N_{xy}D_{y}^{\alpha}w_{0})$

$$+ \mathfrak{D}_{y}^{\alpha}(Q_{yz} + N_{xy}D_{x}^{\alpha}w_{0} + N_{yy}D_{y}^{\alpha}w_{0}) + F_{z} = \rho h \frac{\partial^{2}w_{0}}{\partial t^{2}}$$
 (17c)

$$\mathfrak{D}_{x}^{\alpha} M_{xx} + \mathfrak{D}_{y}^{\alpha} M_{xy} - Q_{xz} + M_{\theta_{x}} = \frac{\rho h^{3}}{12} \frac{\partial^{2} \theta_{x}}{\partial t^{2}}$$
 (17d)

$$\mathfrak{D}_x^{\alpha} M_{xy} + \mathfrak{D}_y^{\alpha} M_{yy} - Q_{yz} + M_{\theta_y} = \frac{\rho h^3}{12} \frac{\partial^2 \theta_y}{\partial t^2}$$
 (17e)

where $\{N_{xx}, N_{yy}, N_{xy}\}$ are the in-plane stress resultants, $\{Q_{xz}, Q_{yz}\}$ are the transverse shear stress resultants, and $\{M_{xx}, M_{yy}, M_{xy}\}$ are the moment resultants. The Dirichlet boundary conditions are obtained as:

$$\delta u_0 = 0, \ \delta v_0 = 0, \ \delta w_0 = 0, \ \delta \theta_x = 0, \ \delta \theta_y = 0 \ \forall \ \partial \Omega_x \cup \partial \Omega_y$$
 (18a)

and the Neumann boundary conditions are obtained as:

$$\begin{split} I_{x}^{1-\alpha}N_{xx} &= \hat{F}_{x}, \ I_{x}^{1-\alpha}N_{xy} = T\hat{F}_{y}, \ I_{x}^{1-\alpha}(Q_{xz} + \mathcal{N}_{xx}) = \hat{F}_{z}, \\ I_{x}^{1-\alpha}M_{xx} &= \hat{M}_{\theta_{x}}, \ I_{x}^{1-\alpha}M_{xy} = \hat{M}_{\theta_{y}} \ \forall \ \partial \Omega_{x} \end{split} \tag{18b}$$

$$I_{y}^{1-\alpha}N_{xy} = \hat{F}_{x}, \ I_{y}^{1-\alpha}N_{yy} = \hat{F}_{y}, \ I_{y}^{1-\alpha}(Q_{yz} + \mathcal{N}_{yy}) = \hat{F}_{z},$$

$$I_{y}^{1-\alpha}M_{xy} = \hat{M}_{\theta_{y}}, \ I_{y}^{1-\alpha}M_{yy} = \hat{M}_{\theta_{y}} \ \forall \ \partial \Omega_{y}$$
(18c)

where $\mathcal{N}_{xx} = N_{xx} D_x^a w_0 + N_{xy} D_y^a w_0$ and $\mathcal{N}_{yy} = N_{xy} D_x^a w_0 + N_{yy} D_y^a w_0$. The different stress and moment resultants in the above governing equations are defined analogously to the classical (local) formulation as:

$$\{N_{xx}, N_{yy}, N_{xy}, Q_{xz}, Q_{yz}\} = \int_{-\frac{h}{2}}^{\frac{h}{2}} \{(\sigma_{xx}), (\sigma_{yy}), \sigma_{xy}, K_s \sigma_{xz}, K_s \sigma_{yz}\} dz \quad (19a)$$

$$\{M_{xx}, M_{yy}, M_{xy}\} = \int_{-\frac{h}{2}}^{\frac{h}{2}} \{-z\sigma_{xx}, -z\sigma_{yy}, -z\sigma_{xy}\} dz$$
 (19b)

where K_s is the shear correction factor. As evident from Eq. (14), the thermal effects are accounted for via the stress and moment resultants. For further clarity, we have encircled these terms in the above equation. Finally, the Riesz fractional integral $I_{x_j}^{1-\alpha}(\cdot)$ in the governing equations is defined as:

$$I_{x_{i}}^{1-\alpha}\psi = \frac{1}{2}\Gamma(2-\alpha)\left[l_{B_{x}}^{\alpha-1}\left({}_{x-l_{B_{x}}}I_{x}^{1-\alpha}\psi\right) - l_{A_{x}}^{\alpha-1}\left({}_{x}I_{x+l_{A_{x}}}^{1-\alpha}\psi\right)\right]$$
(20)

where $_{x-l_{B_x}}I_x^{1-\alpha}\psi$ and $_xI_{x+l_{A_x}}^{1-\alpha}\psi$ are the left-handed and right-handed Riesz integrals to the order α of an arbitrary function ψ , respectively. The fractional-order derivative $\mathfrak{D}^{\alpha}(\cdot)$ is the first-order derivative of the Riesz integral:

$$\mathfrak{D}_{x_{i}}^{\alpha}\psi = D_{x}^{1} \left[I_{x_{i}}^{1-\alpha}\psi \right] \tag{21}$$

Note that $\mathfrak{D}_{x_j}^{\alpha}(\cdot)$ and $I_{x_j}^{1-\alpha}(\cdot)$ are defined above the interval $(x_j-l_{B_j},x_j+l_{A_j})$ unlike the RC fractional derivative $\mathcal{D}_x^{\alpha}(\cdot)$ in Eq. (2) which is defined over $(x_j-l_{A_j},x+l_{B_j})$. This is a direct result of the variational simplifications [39,50].

The nonlinear thermomechanical governing equations given in Eq. (17) deserve some additional remarks. As highlighted in Eq. (19), the presence of the thermal field variables in the expressions for stress resultants introduces the thermal field variables into the governing equations. Absence of the external thermal field ($\theta(x) = 0$) reduces the model to a purely mechanical geometrically nonlinear model as presented in [42,45]. Further, note that the nonlinear nature of the model developed in this study is clearly evident from the transverse

governing equation (Eq. (17c)). The in-plane stress resultants in the transverse governing equations introduces the coupling of axial and transverse field variables. Ignoring the nonlinear terms in the transverse governing equation provides the linear thermoelastic fractional-order model for nonlocal plates. Finally, for $\alpha=1.0$, the classical (local) thermoelastic Mindlin plate model is recovered.

4. Results and discussion

In this section, we analyze the effect of thermal loads on the *static* postbuckling and nonlinear bending response of the nonlocal plate. In all simulations, we consider an isotropic Aluminum plate having Young's modulus E=70 GPa, Poisson's ratio v=1/3, and coefficient of thermal expansion $\alpha_0=2.3\times 10^{-5}$ K⁻¹ [49]. Further, we consider a square plate having dimensions L=B=1 m and thickness h=L/25. The fractional parameters (i.e. the order α and the nonlocal length scales) are not fixed *a priori* and are used as free parameters to study the effect on the plate's response. We have assumed an isotropic and symmetric horizon of nonlocality such that $l_{A_j}=l_{B_j}=l_f$ for points sufficiently far from the boundaries. Recall from Section 2 that this symmetry is broken for points close to the plate boundaries (see Fig. 1).

Before proceeding to present the numerical results, we discuss some details of the numerical technique adopted to simulate the fractional-order thermomechanical formulation. The nonlocal and nonlinear thermoelastic governing equations are numerically solved using the fractional-order finite element method (f-FEM) developed in [39, 411. The f-FEM converts the nonlinear fractional-order governing equations into a set of nonlinear algebraic equations that are solved using an incremental-iterative Newton-Raphson method. We set a tolerance of $10^{-4} \times h$ for the \mathbb{L}^2 norm of the difference between displacements obtained in successive iterations. For tracing the nonlinear equilibrium path in both the postbuckling and bending analyses, we used an arc-length continuation method. This algorithm is discussed in detail in [42,45] and, for the sake of brevity, details are not repeated here. The bending and shear stiffness matrices are integrated using the Gauss quadrature numerical integration, with 2×2 and 1×1 Gauss quadrature points, respectively. This choice of the reduced-order Gauss quadrature integration for the shear stiffness matrices is to avoid the shear locking effects in the numerical simulation of Mindlin plates [49]. To ensure that the results obtained are fully converged upon refinement of the mesh, we set the *dynamic rate of convergence* as $\mathcal{N}_x \times \mathcal{N}_y = (l_f/l_{e_x} \times l_f/l_{e_x})$ l_f/l_{e_v}) = 12 × 12 ($l_{e_x} \times l_{e_v}$ denotes the size of a mesh element). This guarantees that the $\hat{\mathbb{L}}^1$ norm of the difference between displacements obtained from successive refinements in the mesh, is less than 2% [41].

Additionally, we have made the following assumptions in simulating the thermomechanical response of the nonlocal plates. First, we assumed that the mechanical constants of the nonlocal plate are isothermal, that is they do not vary with the externally applied thermal field. While the latter assumption can be circumvented via appropriate changes in the constitutive equations (see, for example, [51]), this study focuses primarily on the effects of the thermal loads and of the fractional-order constitutive parameters on the postbuckling and nonlinear bending response of nonlocal plates. Next, we assumed an external thermal field without analyzing the nature of the heat conduction problem or even its source. In other terms, we do not solve the heat conduction equation to obtain the temperature field within the nonlocal plate. We merely note that the heat conduction problem within the nonlocal solid could be considered either in integer- or fractional-order form, depending on the specific details of the heat transfer process [44,52]. While there is an extensive literature on the significance and application of classical integer-order heat conduction formulation, spatial and/or temporal fractional-order heat conduction formulations have been developed and analyzed fairly recently [52]. Time-fractional heat conduction models capture heat conduction in dissipative systems [52]. On the other hand, space-fractional heat conduction allows the modeling of anomalously diffusive heat transfer in

systems that are potentially conservative such as, for example, fractals and porous media [52,53]. Note that the elastodynamic formulation in [52] is based on integer-order (classical) continuum relations. Hence, it appears that there is an opportunity to couple the fractional-order heat conduction formulations [52] with the fractional-order elastodynamic formulation presented in this study, to develop and analyze a fully fractional thermoelastic formulation. Notably, a key challenge to the development of the latter comprehensive formulation is the fact that a direct replacement of the classical integer-order derivatives in the heat conduction equation with fractional derivatives violates the second law of thermodynamics [54].

4.1. Postbuckling response

We analyzed the postbuckling response of the nonlocal plate subject to different combinations of thermal and axially compressive loads, as well as different values of the fractional parameters. We highlight that, while the framework presented is general, we have restricted the numerical investigations to some standard choices of loading and boundary conditions. The nonlocal plate was subjected to a uniformly distributed (uniaxial) compressive load P at the boundaries $\hat{x} = \{0, L\}$. Additionally, a uniformly distributed transverse load q_0 was applied on the plate to activate the stable branch of the bifurcated postbuckling response at the critical point [32]. This transverse load plays a role analogous to the geometric imperfections used in postbuckling analysis [55]. The additional load provides a first-order contribution to deformation energy, and does not affect the post-buckling response which is a second-order response. Further, the plate was subject to a steady state uniform temperature distribution across the thickness, that is, $\theta(x) = \theta_0$ (in K) [47]. Recall that $\theta(x)$ indicates the temperature perturbation, that is above the reference temperature. Finally, we consider two sets of boundary conditions. In each case all the edges of the plate are either simply supported (denoted as SSSS-01) or clamped (denoted as CCCC-01). The loaded edges in each case are allowed to move in the direction of the uniaxial compressive forces. Mathematically, these conditions are given by [32,47]:

SSSS-01:
$$\begin{cases} \hat{x} = \{0, L\} : v_0 = w_0 = \theta_y = 0 \\ \hat{y} = \{0, B\} : u_0 = w_0 = \theta_x = 0 \end{cases}$$
 (22a)

CCCC-01:
$$\begin{cases} \hat{x} = \{0, L\} : v_0 = w_0 = \theta_x = \theta_y = 0 \\ \hat{y} = \{0, B\} : u_0 = v_0 = w_0 = \theta_x = \theta_y = 0 \end{cases}$$
 (22b)

The above described loading conditions are simulated using the nonlinear f-FEM [42] and the results obtained are reported in Fig. 3 in terms of the following non-dimensionalized variables:

$$\overline{P} = P \times \frac{L^2}{\pi^2 E h^3} \tag{23a}$$

$$\overline{w} = \max(w_0) \times \frac{1}{h} \tag{23b}$$

The transverse load q_0 (mimicking the imperfection) is taken as $q_0=0.1E(h/L)^4$ which is insignificant (to the $\mathcal{O}(3)$) when compared to the compressive axial loads. In Fig. 3, we have compared the post-buckling response of the plates for different values of the loading conditions and fractional-order constitutive parameters. In regards to the fractional-order constitutive parameters, we varied the fractional-order $\alpha \in [0.7,1]$ while fixing the length scale as $l_f=0.5L$ in Fig. 3a.1, b.1. In Fig. 3a.2, b.2, we fixed the order as $\alpha=0.9$ and varied the length scale $l_f \in [0.3L,0.5L]$. Further, the different color-coded surfaces correspond to different values of the thermal load θ_0 . To improve the visualization of the postbuckling curves, we have projected selected lines from these surfaces onto the $\overline{w}-\overline{P}$ plane. These projected curves correspond to the thermomechanical postbuckling response of the nonlocal plate for a fixed value of θ_0 and a selected combination of α and l_f . Before proceeding further, we emphasize that the specific

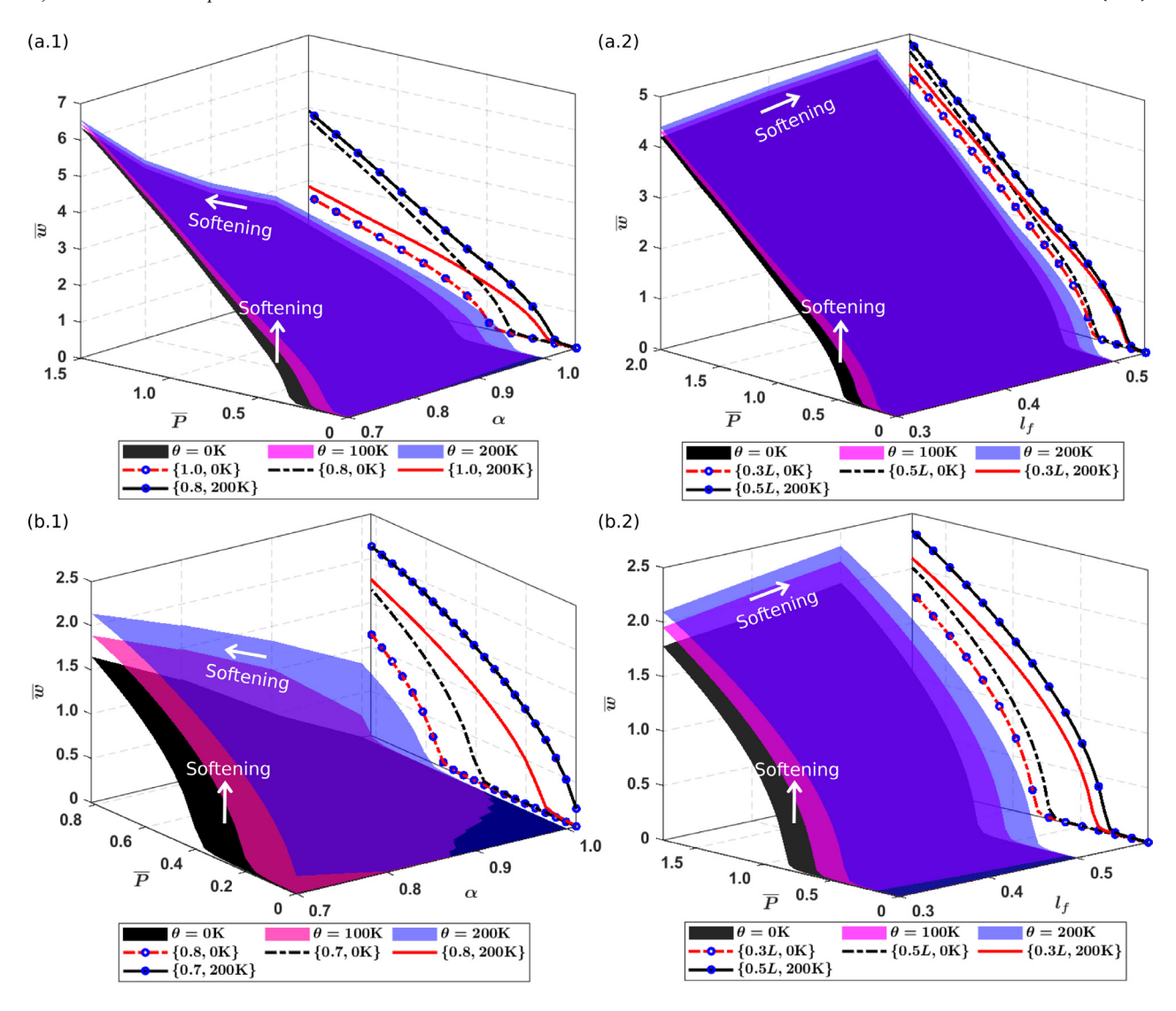


Fig. 3. Postbuckling response measured in terms of the maximum transverse displacement (which can occur at different physical points) of the nonlocal plate subject to combined thermal and axial loads. The plate is (a) simply supported at all its edges (SSSS-01) and (b) clamped at all its edges (CCCC-01). The response is parameterized (a.1,b.1) for different values of the fractional-order α for a fixed length scale $l_f = 0.5L$, and (a.2,b.2) for different the length scale l_f values and a fixed fractional-order $\alpha = 0.9$. With respect to the equilibrium curves projected on the plane $\overline{w} - \overline{P}$, the legend reports the values of the order and of the thermal load for (a.1,b.1), and the values of the length scale and of the thermal load for (a.2,b.2). Further, the markers in some of the equilibrium curves are only used to facilitate the distinction between different curves. They do not indicate the successive values of \overline{P} used within the numerical simulation. (For interpretation of the references to colour in this figure legend, the reader is referred to the web version of this article.)

numerical values of the different parameters do not affect the generality of the conclusions presented below. However, some caution is required in selecting the value of the fractional-order α . As reported in several studies, there exists a critical value for the fractional-order (α_c) below which the fractional-order model of nonlocality breaks down [38–40]. We found that the critical value is $\alpha_c\approx 0.4$, similar to [40]. Notably, this critical value also depends on the relative ratio: l_f/L , that is the size of the horizon of nonlocality relative to the characteristic dimension of the structure. It was noted that, for l_f/L close to 1, the critical value of α increases to $\alpha_c\approx 0.3$. While the fractional-order model is mathematically (and numerically) still consistent, from a physical perspective, for small values of α , the material exhibits a large degree of softening that leads to physically inconsistent results. Detailed qualitative discussions on this aspect can be found in [38–40].

A detailed analysis of the numerical results in Fig. 3 leads to the following conclusions: $\$

• An increase in the degree of nonlocality (by reducing the order α and/or increasing the length scale l_f), for a fixed loading

condition, leads to a consistent softening of the structure irrespective of the choice of boundary conditions. In other terms, the postbuckling stability of the structure reduces with an increase in the degree of nonlocality. This conclusion emerges in Fig. 3 by following the response \overline{w} for either decreasing α or increasing l_f for a fixed θ_0 and \overline{P} .

• Increasing the thermal load, for a fixed combination of α , l_f , and \overline{P} , leads to a *consistent softening* of the structure. In other terms, an increase in the temperature of the plate reduces its structural stability which is consistent with classical predictions and experimental evidence [1,2,18,47]. This conclusion emerges by following the \overline{w} axis across the different isothermal surfaces.

For a more complete analysis, we also present the postbuckled shapes of the plates subjected to the different loading conditions. We consider the postbuckled shape of the mid-plane of the simply supported plates, for increasing values of the axial compression load \overline{P} and different thermal loads $\theta \in \{0,200\}$ K. These results are presented in Fig. 4. In each case, the nonlocal response obtained for a plate with

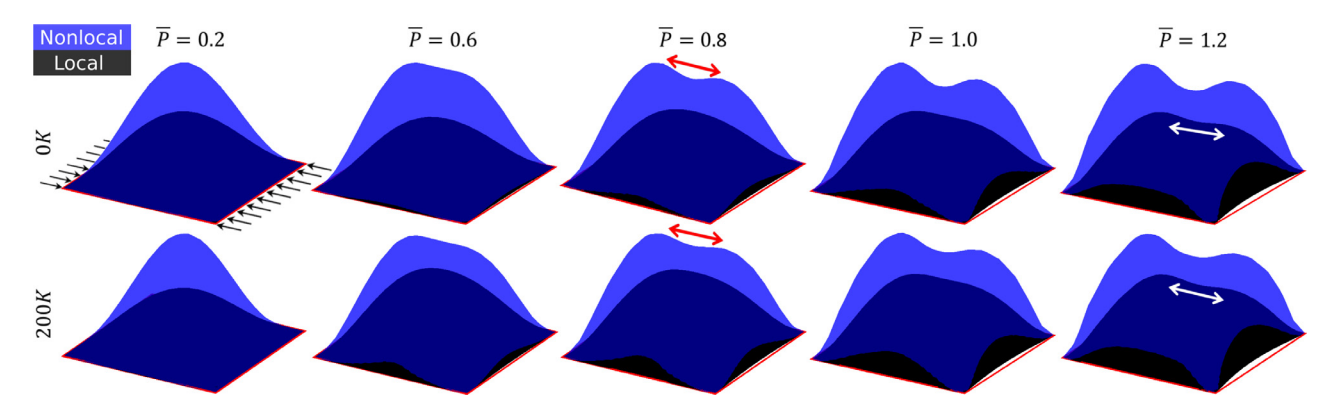


Fig. 4. The postbuckled shape of the midplane of a simply supported plate is presented for increasing axial load \overline{P} and two values of the thermal load $\theta \in \{0,200\}$ K. The direction of the axial compressive load is indicated for the first case. The rectangle at the bottom of each plot corresponds to the undeformed midplane of the plate. For each combination of $\{\overline{P},\theta\}$, we have compared the local response (obtained for $\alpha=1$) against a nonlocal response (obtained for $\alpha=0.8$ and $I_f=0.5L$). Note that the transition from the first mode of buckling to a higher mode occurs for a lower load in case of the nonlocal plate due to its lower stiffness (when compared to a local plate) [41,42].

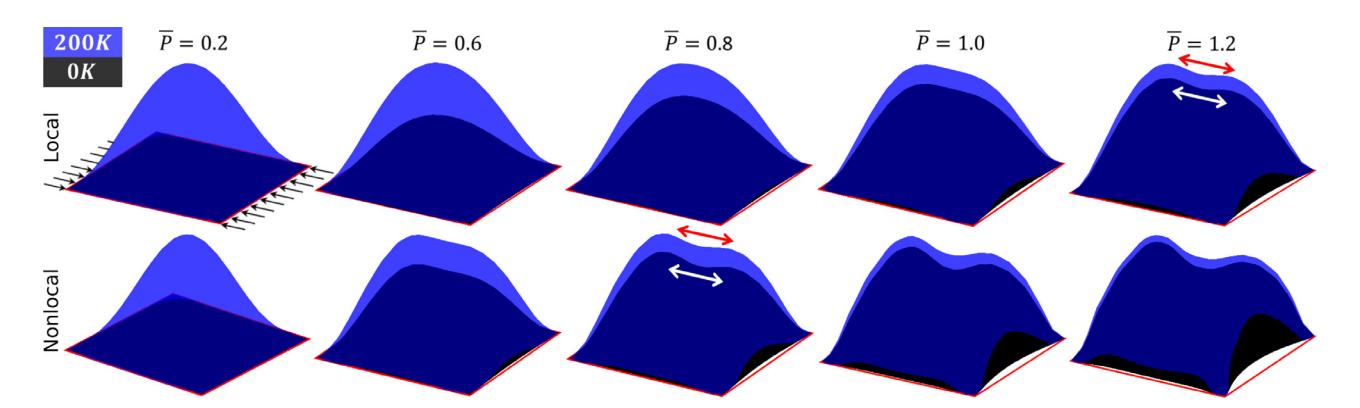


Fig. 5. The postbuckled shape of the midplane of a simply supported plate is presented for a local and a nonlocal ($\alpha = 0.8, l_f = 0.5L$) plate subject to increasing axial loads. The direction of the axial compressive load is indicated for the first case. The rectangle at the bottom of each plot corresponds to the undeformed midplane of the plate. For each case, we have compared the response at two thermal loads: $\theta \in \{0,200\}$ K. As evident, increase in the thermal load results in an enhanced softening of the structure. It also appears that the assumed range of thermal loads do not affect the particular mode of postbuckling, for a fixed axial load and a fixed degree of nonlocality.

the fractional parameters $\alpha = 0.8$ and $l_f = 0.5L$ is compared with the response of the corresponding local plate. We do not present the specific values of the transverse displacement since they marginally affect the overall conclusions. In addition to the consistent softening of the plate, visible by the larger transverse deformation of the nonlocal plate, some additional interesting observations follow from the results in Fig. 4. It appears that, both the local and the nonlocal plates gradually shift to a higher mode of buckling with the increasing axial load \overline{P} . The appearance of the higher order mode leads to a transition in the material point having maximum displacement, that is, from the center of the plate to two symmetrical points lying along the direction of the axial forces. For better visualization, we have indicated this transition by the double-headed red and white arrows. The shift in the mode of buckling occurs for a lower value of \overline{P} for the nonlocal plate, when compared to the local plate. This is a direct result of the lower stiffness of the nonlocal plate. Further, we analyzed the effect of the thermal load on the deformed shape of the SSSS-01 plate, for a fixed degree of nonlocality. These results are presented in Fig. 5 and they establish that an increase in the thermal load results in an increased softening of the structure. It also appears that the given range of thermal loads do not affect the particular mode of postbuckling, for a fixed axial load and a fixed degree of nonlocality.

The consistent softening response predicted by the fractional-order formulation is a significant result when compared to the often incoherent predictions of classical (integer-order) strain-driven integral approaches. More specifically, the results obtained from the fractional-order approach are free from the typically troubling behavior like hardening of the structure and even the absence of nonlocal effects

noted via strain-driven methods, under selected loading conditions [24, 25]. To clarify this point: hardening effects in nonlocal structures are consistent with the physics of the problem but should not be predicted following classical strain-driven integral approaches. It is worth noting that the inconsistency resulting from mathematical ill-posedness of the strain-driven approach was addressed via the stress-driven nonlocal approach [25]. However, stress-driven approach exhibits some important challenges connected to numerical implementation and thermal analysis. Recall from Section 1 that the stress-driven approach only admits analytical solution techniques [25,30]. While this approach offers interesting analytical insights, it prevents the application of the stressdriven formulation to the analysis of complex geometry (even plates) subject to general loading conditions. In fact, it appears that the stressdriven approach has not yet been applied to analyze geometrically nonlinear response of nonlocal structures. Further, under combined thermomechanical loads the stress-driven approach predicts an initial softening and a gradual switch to stiffening with increasing degree of nonlocality [30]. On the contrary, the fractional-order model presents consistent predictions under combined thermomechanical loads, as evident from the results presented above.

Due to these complexities associated with either strain- or stress-driven integral approaches, previous studies on the postbuckling analysis of nonlocal structures have invariably relied on gradient-based approaches to nonlocality. The above discussion also suggests that the fractional-order approach (which bears some resemblance to the integral approaches) presents a promising alternative to the analysis of postbuckling of nonlocal structures. Notably, gradient-based approaches result in consistent thermomechanical predictions [7,8,19].

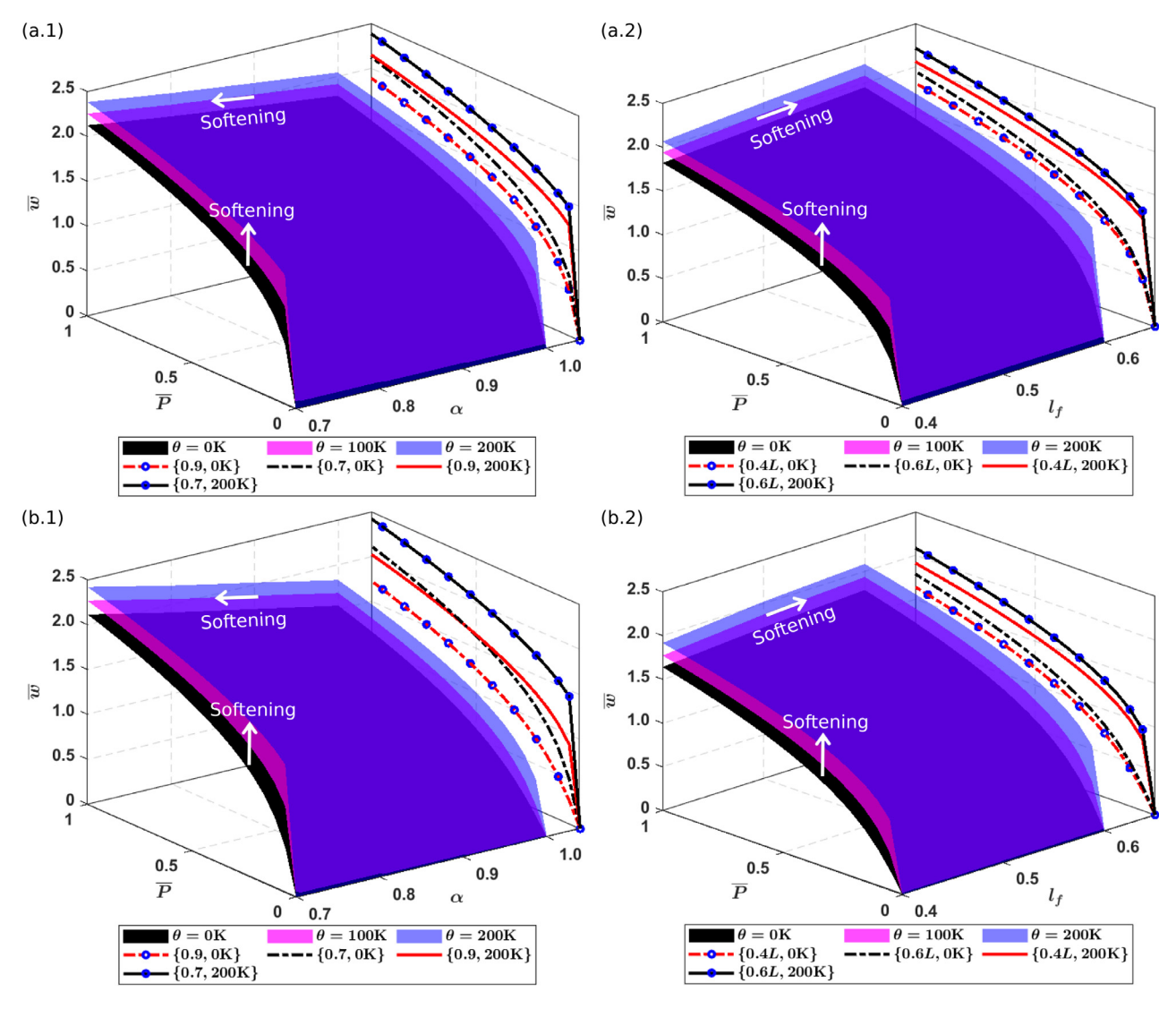


Fig. 6. Nonlinear bending response measured in terms of the non-dimensionalized displacement at the center point of the nonlocal plate subject to combined transverse and thermal loads. The plate is (a) simply supported at all its edges (SSSS-02) and (b) clamped at all its edges (CCCC-02). The response is parameterized (a.1,b.1) for different values of the fractional-order α for a fixed length scale $l_f = 0.5L$, and (a.2,b.2) for different length scale l_f values and a fixed fractional-order $\alpha = 0.9$. With respect to the equilibrium curves projected on the plane $\overline{w} - \overline{P}$, the legend reports the values of the order and of the thermal load for (a.1,b.1), and the values of the length scale and of the thermal load for (a.2,b.2). Further, the markers in some of the equilibrium curves are only used to facilitate the distinction between different curves. They do not indicate the successive values of \overline{P} used within the numerical simulation.

However, some difficulties arise while extending gradient-based approaches to dynamic analysis. As discussed in detail in [26], gradient based approaches require additional acceleration gradient terms in the constitutive formulation to ensure both well-posedness and causality. Remarkably, a recent extension of the fractional-order continuum approach demonstrated how both the integral and the gradient formulations can be unified into a stable, well-posed, and causal framework without requiring additional acceleration gradient terms [50]. This was achieved via a multifractional (or multifractal) extension of the deformation energy in Eq. (6) [50]. Hence, it appears that the application of the unified fractional-order approach [50] to the postbuckling of nonlocal structures is a promising extension of the current study.

4.2. Bending response

The nonlinear and nonlocal formulation was also applied to analyze the nonlinear bending response of the nonlocal plate. The effects of different combinations of thermal and transverse mechanical loads as well as different fractional parameters are investigated, similar to the approach followed in Section 4.1. For the specific numerical analyses,

the plate was subject to a uniformly distributed transverse load P and a uniform temperature distribution $\theta(\mathbf{x}) = \theta_0$ (in K). No axial forces were applied in this study. The simply supported (denoted as SSSS-02) and clamped (denoted as CCCC-02) boundary conditions were used. Unlike for the postbuckling analysis (see Eq. (22)), in this case the boundaries do not allow for any in-plane displacement. Mathematically, these conditions are given as [49]:

SSSS-02:
$$\begin{cases} \hat{x} = \{0, L\} : u_0 = v_0 = w_0 = 0 \\ \hat{y} = \{0, B\} : u_0 = v_0 = w_0 = 0 \end{cases}$$
 (24a)

CCCC-02:
$$\begin{cases} \hat{x} = \{0, L\} : u_0 = v_0 = w_0 = \theta_x = \theta_y = 0 \\ \hat{y} = \{0, B\} : u_0 = v_0 = w_0 = \theta_x = \theta_y = 0 \end{cases}$$
 (24b)

Once again, the solution was obtained using the nonlinear f-FEM and the results are reported in Fig. 6. The transverse load P and the transverse displacement are non-dimensionalized using Eq. (23). In Fig. 6, we have compared the nonlinear bending response of the plates for different boundary conditions and different values of the fractional-order constitutive parameters. In Fig. 6a.1, b.1, we varied the fractional order $\alpha \in [0.7, 1]$ while fixing the length scale $l_f = 0.5L$.

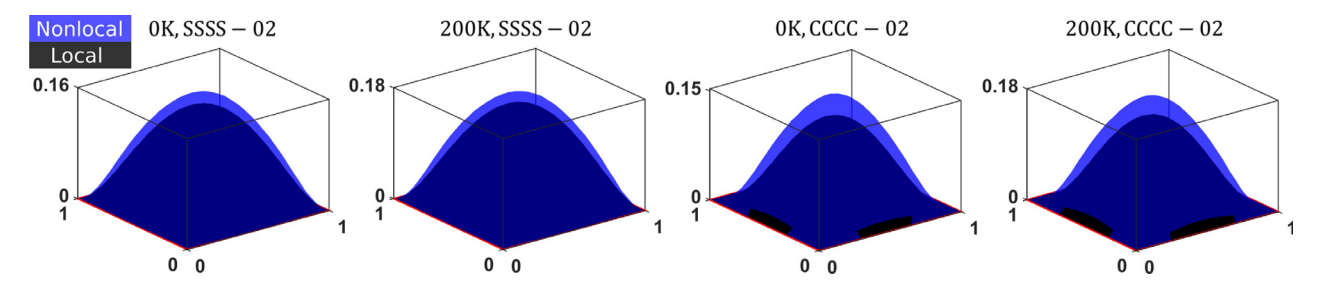


Fig. 7. The deformed shape of the mid-plane of a local and a nonlocal ($\alpha=0.8, l_f=0.5L$) plate subject to a transverse load $\overline{P}=1$, different thermal loads $\theta\in\{0,200\}$ K, and different boundary conditions. The rectangle at the bottom of each plot corresponds to the undeformed mid-plane of the plate.

In Fig. 6a.2, b.2, we fixed the order as $\alpha=0.9$ and varied the length scale $l_f\in[0.4L,0.6L]$. Similar to the results presented in Section 4.1, the iso-surfaces in these figures correspond to different values of the thermal load θ_0 . Selected lines from these iso-surfaces were projected onto the $\overline{w}-\overline{P}$ plane to facilitate the visualization. These projected curves correspond to the bending response of the nonlocal plate for a fixed value of the thermal load θ_0 and a selected combination of α and l_f . Additionally, we have presented the deformed shape of the plates for selected cases in Fig. 7.

As evident from Figs. 6, 7, the conclusions drawn for the thermome-chanical postbuckling response directly extend to the nonlinear bending response. Key conclusions include the consistent softening response of the nonlocal structure with either increasing degree of nonlocality or increasing thermal load, irrespective of the loading conditions. We highlight that a sharp change in the curvature noted for the higher thermal loads is due to the selection of specific values of the transverse load. More specifically, the transverse load corresponding to the point of inflection, is the load applied immediately after $\overline{P}=0$. While the curves (and the corresponding iso-surfaces) can be made smoother by using a finer discretization of the load increments, the general nature of the response and the overall conclusions would not be altered.

5. Conclusions

This study presented a fractional order formulation capable of capturing the effect of nonlocality on the nonlinear thermoelastic response of thin plate structures. Particular emphasis was given to the development of a mathematically and physically consistent formulation. The positive-definite nature of the fractional-order nonlocal continuum formulation combined with its thermodynamic consistency enabled the use of an energy-based method. The combination of these factors yielded a powerful approach to address key challenges in the application of existing classical (integer-order) nonlocal formulations. First, in the case of postbuckling analyses, the fractional formulation allowed for an extension of the classical Koiter's asymptotic approach to analyze the impact of nonlocal interactions on the nature of bifurcation and post-critical response of thin plates. Second, it enabled the development of an accurate finite element formulation to simulate the nonlinear system subject to any combination of thermomechanical load and boundary conditions. Noteworthy is the fact that, the mathematical well-posedness of the fractional-order formulation (a direct result of its positive-definite nature) ensures predictions of the response of the nonlocal structures that are consistent and free from paradoxical boundary and loading effects. Results established that nonlocal structures exhibit a consistent softening behavior following the increasing degree of nonlocality and the magnitude of thermal loads. This effect translates into lower stability when subject to axially compressive loads and into higher displacements when subject to transverse bending loads. The mathematical well-posed nature, the thermodynamic consistency, and the ability to integrate nonlinear displacements combined with the possibility to employ a finite element method to achieve a numerical solution provide significant advancements to the state of the art of nonlinear thermoelastic analysis of slender structures. Results also suggest

that fractional order formulations of structural elements can provide a powerful and reliable foundation for the simulation of structures subject to complex loading and response conditions.

CRediT authorship contribution statement

Sansit Patnaik: Conceptualization, Methodology, Software, Formal analysis, Writing - original draft, Visualization. Sai Sidhardh: Conceptualization, Methodology, Software, Formal analysis, Writing - original draft, Visualization. Fabio Semperlotti: Conceptualization, Methodology, Formal analysis, Writing - original draft, Writing - review & editing, Visualization, Supervision, Project administration, Funding acquisition.

Declaration of competing interest

The authors declare that they have no known competing financial interests or personal relationships that could have appeared to influence the work reported in this paper.

Acknowledgments

The authors gratefully acknowledge the financial support of the Defense Advanced Research Project Agency (DARPA), USA under the grant #D19AP00052, and the National Science Foundation (NSF), USA under the grant MOMS, USA #1761423 and DCSD, USA #1825837. The content and information presented in this manuscript do not necessarily reflect the position or the policy of the government. The material is approved for public release; distribution is unlimited.

References

- K.D. Murphy, L.N. Virgin, S.A. Rizzi, Experimental snap-through boundaries for acoustically excited, thermally buckled plates, Exp. Mech. 36 (4) (1996) 312–317.
- [2] P. Marzocca, S.A. Fazelzadeh, M. Hosseini, A review of nonlinear aero-thermoelasticity of functionally graded panels, J. Therm. Stresses 34 (5–6) (2011) 536–568
- [3] J. Romanoff, J.N. Reddy, J. Jelovica, Using non-local timoshenko beam theories for prediction of micro-and macro-structural responses, Compos. Struct. 156 (2016) 410–420.
- [4] H. Zhu, S. Patnaik, T.F. Walsh, B.H. Jared, F. Semperlotti, Nonlocal elastic metasurfaces: Enabling broadband wave control via intentional nonlocality, Proc. Natl. Acad. Sci. 117 (42) (2020) 26099–26108.
- [5] G. Alotta, M. Di Paola, F.P. Pinnola, M. Zingales, A fractional nonlocal approach to nonlinear blood flow in small-lumen arterial vessels, Meccanica (2020) 1–16.
- [6] O.S. Hussein, S.B. Mulani, Nonlinear aeroelastic stability analysis of in-plane functionally graded metal nanocomposite thin panels in supersonic flow, Thin-Walled Struct. 139 (2019) 398–411.
- [7] Y. Xu, H.S. Shen, C.L. Zhang, Nonlocal plate model for nonlinear bending of bilayer graphene sheets subjected to transverse loads in thermal environments, Compos. Struct. 98 (2013) 294–302.
- [8] H.S. Shen, Y. Xu, C.L. Zhang, Prediction of nonlinear vibration of bilayer graphene sheets in thermal environments via molecular dynamics simulations and nonlocal elasticity, Comput. Methods Appl. Mech. Engrg. 267 (2013) 458–470.

- [9] A.R. Ashoori, S.A.S. Vanini, Nonlinear bending, postbuckling and snap-through of circular size-dependent functionally graded piezoelectric plates, Thin-Walled Struct. 111 (2017) 19–28.
- [10] R. Basutkar, S. Sidhardh, M.C. Ray, Static analysis of flexoelectric nanobeams incorporating surface effects using element free Galerkin method, Eur. J. Mech. A Solids 76 (2019) 13–24.
- [11] C.Y. Wang, T. Murmu, S. Adhikari, Mechanisms of nonlocal effect on the vibration of nanoplates, Appl. Phys. Lett. 98 (15) (2011) 153101.
- [12] S. Nair, Nonlocal Acoustic Black Hole Metastructures: Achieving Ultralow Frequency and Broadband Vibration Attenuation (Ph.D. thesis), Purdue University Graduate School. 2019.
- [13] J.P. Hollkamp, M. Sen, F. Semperlotti, Analysis of dispersion and propagation properties in a periodic rod using a space-fractional wave equation, J. Sound Vib. 441 (2019) 204–220.
- [14] S. Patnaik, F. Semperlotti, A generalized fractional-order elastodynamic theory for non-local attenuating media, Proc. R. Soc. Lond. Ser. A Math. Phys. Eng. Sci. 476 (2238) (2020) 20200200.
- [15] D. Capecchi, G. Ruta, P. Trovalusci, Voigt and Poincaré's mechanistic-energetic approaches to linear elasticity and suggestions for multiscale modelling, Arch. Appl. Mech. 81 (11) (2011) 1573–1584.
- [16] M. Shaat, E. Ghavanloo, S.A. Fazelzadeh, Review on nonlocal continuum mechanics: Physics, material applicability, and mathematics, Mech. Mater. (2020) 103587
- [17] L.E. Shen, H.-S. Shen, C.-L. Zhang, Nonlocal plate model for nonlinear vibration of single layer graphene sheets in thermal environments, Comput. Mater. Sci. 48 (3) (2010) 680–685.
- [18] S. Zandekarimi, B. Asadi, M. Rahaeifard, Size dependent thermal buckling and postbuckling of functionally graded circular microplates based on modified couple stress theory, J. Therm. Stresses 41 (1) (2018) 1–16.
- [19] R. Kolahchi, H. Hosseini, M.H. Fakhar, R. Taherifar, M. Mahmoudi, A numerical method for magneto-hygro-thermal postbuckling analysis of defective quadrilateral graphene sheets using higher order nonlocal strain gradient theory with different movable boundary conditions, Comput. Math. Appl. 78 (6) (2019) 2018–2034
- [20] M.H. Jalaei, Ö. Civalek, A nonlocal strain gradient refined plate theory for dynamic instability of embedded graphene sheet including thermal effects, Compos. Struct. 220 (2019) 209–220.
- [21] A. Kazemi, R. Vatankhah, Thermal vibration and nonlinear buckling of micro-plates under partial excitation, Eur. J. Mech. A Solids (2020) 104185.
- [22] A.C. Eringen, D.G.B. Edelen, On nonlocal elasticity, Internat. J. Engrg. Sci. 10 (3) (1972) 233–248.
- [23] S.A.M. Ghannadpour, F. Moradi, F. Tornabene, Exact analytical solutions to the problem of relative post-buckling stiffness of thin nonlocal graphene sheets, Thin-Walled Struct. 151 (2020) 106712.
- [24] N. Challamel, C.M. Wang, The small length scale effect for a non-local cantilever beam: A paradox solved, Nanotechnology 19 (34) (2008) 345703.
- [25] G. Romano, R. Barretta, M. Diaco, F.M. de Sciarra, Constitutive boundary conditions and paradoxes in nonlocal elastic nanobeams, Int. J. Mech. Sci. 121 (2017) 151–156.
- [26] H. Askes, E.C. Aifantis, Gradient elasticity in statics and dynamics: An overview of formulations, length scale identification procedures, finite element implementations and new results, Int. J. Solids Struct. 48 (13) (2011) 1962–1990.
- [27] F. Balta, E.S. Şuhubi, Theory of nonlocal generalised thermoelasticity, Internat. J. Engrg. Sci. 15 (9–10) (1977) 579–588.
- [28] C. Polizzotto, Nonlocal elasticity and related variational principles, Int. J. Solids Struct. 38 (42–43) (2001) 7359–7380.
- [29] P. Lu, P.Q. Zhang, H.P. Lee, C.M. Wang, J.N. Reddy, Non-local elastic plate theories, Proc. R. Soc. A 463 (2088) (2007) 3225–3240.
- [30] R. Barretta, M. Čanadija, R. Luciano, F.M. de Sciarra, Stress-driven modeling of nonlocal thermoelastic behavior of nanobeams, Internat. J. Engrg. Sci. 126 (2018) 53–67.

- [31] W.T. Koiter, Over de Stabiliteit van het Elastisch Evenwicht (Ph.D. thesis), Technische Universiteit Delft. 1945.
- [32] B. Budiansky, Theory of buckling and post-buckling behavior of elastic structures, in: Advances in Applied Mechanics, Vol. 14, Elsevier, 1974, pp. 1–65.
- [33] K.A. Lazopoulos, Non-local continuum mechanics and fractional calculus, Mech. Res. Commun. 33 (6) (2006) 753–757.
- [34] M. Di Paola, G. Failla, A. Pirrotta, A. Sofi, M. Zingales, The mechanically based non-local elasticity: An overview of main results and future challenges, Phil. Trans. R. Soc. A 371 (1993) (2013) 20120433.
- [35] A. Carpinteri, P. Cornetti, A. Sapora, Nonlocal elasticity: An approach based on fractional calculus, Meccanica 49 (11) (2014) 2551–2569.
- [36] G. Alotta, M. Di Paola, G. Failla, F.P. Pinnola, On the dynamics of non-local fractional viscoelastic beams under stochastic agencies, Composites B 137 (2018) 102–110.
- [37] C.S. Drapaca, S. Sivaloganathan, A fractional model of continuum mechanics, J. Elasticity 107 (2) (2012) 105–123.
- [38] W. Sumelka, T. Blaszczyk, Fractional continua for linear elasticity, Arch. Mech. 66 (3) (2014) 147–172.
- [39] S. Patnaik, S. Sidhardh, F. Semperlotti, A ritz-based finite element method for a fractional-order boundary value problem of nonlocal elasticity, Int. J. Solids Struct. 202 (2020) 398–417.
- [40] S. Sidhardh, S. Patnaik, F. Semperlotti, Geometrically nonlinear response of a fractional-order nonlocal model of elasticity, Int. J. Nonlinear Mech. 125 (2020) 103529.
- [41] S. Patnaik, S. Sidhardh, F. Semperlotti, Fractional-order models for the static and dynamic analysis of nonlocal plates, Commun. Nonlinear Sci. Numer. Simul. 95 (2020) 105601.
- [42] S. Patnaik, S. Sidhardh, F. Semperlotti, Geometrically nonlinear analysis of nonlocal plates using fractional calculus, Int. J. Mech. Sci. 179 (2020) 105710.
- [43] S. Sidhardh, S. Patnaik, F. Semperlotti, Thermodynamics of fractional-order nonlocal continua and its application to the thermoelastic response of beams, Eur. J. Mech. A Solids (2021) 104238.
- [44] S. Sidhardh, S. Patnaik, F. Semperlotti, Fractional-order structural stability: Formulation and application to the critical load of slender structures, 2020, arXiv preprint arXiv:2008.11528.
- [45] S. Sidhardh, S. Patnaik, F. Semperlotti, Analysis of the post-buckling response of nonlocal plates via fractional order continuum theory, J. Appl. Mech. 88 (2020) 1–22.
- [46] M. Tuna, M. Kirca, P. Trovalusci, Deformation of atomic models and their equivalent continuum counterparts using Eringen's two-phase local/nonlocal model, Mech. Res. Commun. 97 (2019) 26–32.
- [47] Y.Y. Lee, X. Zhao, J.N. Reddy, Postbuckling analysis of functionally graded plates subject to compressive and thermal loads, Comput. Methods Appl. Mech. Engrg. 199 (25–28) (2010) 1645–1653.
- [48] D. Allman, On the general theory of the stability of equilibrium of discrete conservative systems, Aeronaut. J. 93 (921) (1989) 29–35.
- [49] J.N. Reddy, Theory and Analysis of Elastic Plates and Shells, CRC press, 2006.
- [50] S. Patnaik, S. Sidhardh, F. Semperlotti, Towards a unified approach to nonlocal elasticity via fractional-order mechanics, Int. J. Mech. Sci. 189 (2020) 105992.
- [51] J. Yang, K.M. Liew, Y.F. Wu, S. Kitipornchai, Thermo-mechanical post-buckling of FGM cylindrical panels with temperature-dependent properties, Int. J. Solids Struct. 43 (2) (2006) 307–324.
- [52] Y. Povstenko, Fractional Thermoelasticity, Vol. 219, Springer, 2015.
- [53] S. Buonocore, F. Semperlotti, Tomographic imaging of non-local media based on space-fractional diffusion models, J. Appl. Phys. 123 (21) (2018) 214902.
- [54] L. Vázquez, J. Trujillo, M.P. Velasco, Fractional heat equation and the second law of thermodynamics, Fract. Calc. Appl. Anal. 14 (3) (2011) 334–342.
- [55] N. Yamaki, Postbuckling behavior of rectangular plates with small initial curvature loaded in edge compression—(continued), J. Appl. Mech. 27 (2) (1960) 335–342.